Two-Dimensional Finite Element Modeling for Modeling Tectonic Stress and Strain

G. A. Lyzenga and A. Raefsky
Tracking Systems and Applications Section

Techniques of finite element analysis in two-dimensional plane strain have been applied in this study to problems of geophysics and tectonics. More specifically, the flexibility of the finite element method has been employed to address problems involving geological complexity and fault interactions. In this work the modeling of effective anisotropy in material elastic properties has proven useful in describing the deformation of faulted crustal blocks. The applications of this modeling work to problems of actual tectonics in southern California have been explored. Preliminary models show encouraging agreement with measured tectonic strain in this region, and modeling work has been done to gain an understanding of the stress state in a "locked" fault region with future seismic potential.

I. Introduction

Understanding the tectonic processes which govern the evolution and present state of continental plate boundary regions such as that in Southern California requires the modeling of crustal deformation. In most instances, whether such modeling addresses broad scale "average" tectonic features of a region, or seeks to understand the detailed processes governing single faults or seismic events, it is important to consider the effects of material heterogeneities in influencing the problem.

In practice, the complications of contrasts and variations in geology and rock properties throughout a region may present formidable challenges for modeling crustal stress and strain. While the application of analytic techniques contributes much, and usually provides physical insight into the general features of a given problem, often numerical techniques are required in order to adequately characterize such complex models. In the work described here, one such numerical method, the finite element method, has been employed. In this work, the finite element method is used in a two-dimensional approximation to construct models of Southern California crustal deformation for correlation with geophysical observations, including geodetic strain measurements and seismicity.

By using finite elements, it is possible to solve for stress distributions in problems of linear elasticity and viscous deformation. In the latter case, both steady, time-independent deformation (Stokes flow) and time-dependent viscoelastic deformation are amenable to treatment by these methods. A particular specialization of this technique which is useful in considering strike slip tectonics of the style observed in Southern California, and which is one of the novel contributions of the present study, is the introduction of anisotropic material constitutive properties into the models. As discussed

below, anisotropic properties allow the modeling of regions characterized by many parallel faults in a diffuse "shear zone," using a continuum finite element model.

Also outlined in this report is the relevance of these modeling results to problems of crustal rheology and earthquake-related transient deformation. The interaction of the current modeling with such studies is in both directions, with independent crustal stress/strain studies both supporting and being augmented by the current finite element work. As an example of the former case, crustal effective viscosities derived from seismic deformation studies serve as input to viscous stress models. In the latter case, finite element modeling has been used in the work described below to address the problem of anomalous stresses in the Anza, California, seismic gap.

II. Modeling Techniques

The finite element method has found increasing applications in problems of modeling tectonic stress and strain. Beyond the solution of simple elasticity problems, the utilization of algorithms for the treatment of viscoelastic stress relaxation (e.g., Refs. 1-3) has allowed the consideration of dynamic problems such as post-seismic rebound and rheological flow.

In general terms, the finite element technique is used to solve a given boundary value problem by breaking the problem domain up into a number of smaller elements. The problem of solving for the continuous field of unknown variables reduces to the discrete problem of solving for function values at the nodal points in the element grid. In this discretization, the task of solving the governing differential equations thus becomes a problem of solving simultaneous linear algebraic equations. Therefore, a central feature of standard finite element analysis is the requirement of obtaining the inverse of a large matrix, which has a rank equal to the total number of nodal degrees of freedom, and is generally symmetric and banded.

In principle, the finite element method allows solution of problems in arbitrary complex geometries, with resolution determined by the (variable) grid spacing in a given region. In practice, limitations of two types are evident. Most obvious is that, as the grid grows in size and complexity, the computer time and storage required for assembly and solution of the matrix equations grows intractable. Furthermore, even if extremely complex grids can be handled on a given machine, the complexity of the model may preclude its being useful to constrain observable quantities in terms of a few unique parameters. The former limitation is imposed by computer capability, while the latter reflects the need for methodical modeling procedure.

When considering three-dimensional models of geological problems, both storage and time constraints become serious. This is a result of the matrix column-storage method used for solving the system. For a number of nodal degrees of freedom, the number of operations required for matrix reduction and back-substitution varies as the square of matrix column height (Ref. 4) while storage varies as the first power.

Since two-dimensional grids display such a lower degree of interconnectivity between nodes than a three-dimensional problem of comparable size, the computation time restriction may be largely avoided by considering 2-D problems. In this case, focusing upon methods of expanding the effective memory available to the program can pay off in allowing the solution of very large two-dimensional problems.

In the discussion which follows, we concentrate on the two-dimensional modeling techniques which have been useful in this tectonic simulation work. Among the principles which make up the paradigm of current plate tectonics is the idea that the lithospheric "plates" behave as relatively rigid entities, coupled in a quasi-viscous manner to an underlying asthenosphere. To first order then, on time scales sufficiently long, the lithosphere is considered to be weakly coupled to the underlying mantle. As a result many problems, especially those involving steady deformation and long-term response, may be considered in a two-dimensional "plane stress" approximation.

If the problem to be considered is one of elastic strain, the standard equations governing stress σ_{ij} in linear elasticity apply:

$$\sigma_{i\mu.\mu} = 0 \tag{1a}$$

$$\sigma_{ij} = \lambda u_{\mu,\mu}\,\delta_{ij} + \mu(u_{i,j} + u_{j,i}) \tag{1b}$$

On the other hand, steady Newtonian viscous flow ($R \gg 1$) is governed by the set of equations,

$$\sigma_{i\mu,\mu} = 0 \tag{2a}$$

$$\sigma_{ij} = (-P + \lambda u_{\mu,\mu})\,\delta_{ij} + \eta(u_{i,j} + u_{j,i}) \tag{2b}$$

where

$$P = f(\rho) \text{ (equation of state)} \tag{2c}$$

and

$$\frac{\partial \rho}{\partial t} + (\rho u_{\mu}),\mu = 0 \text{ (continuity)} \tag{2d}$$

In conventional usage, these steady flow equations are used in the case of divergenceless flow, in which case $U_{\mu,\mu} = 0$ and ρ and P are constants. It is apparent through comparison of Eqs. (1) and (2) that in this limit the Newtonian flow equations are identical with those describing incompressible elasticity. Carrying this comparison further, we can see that if $U_{\mu,\mu} \neq 0$ is permitted in the flow equations, perhaps through use of a special form of the equation of state which limits the growth of P with increasing ρ, we obtain equations essentially identical to general linear elasticity, with only the addition of a hydrostatic pressure term to the stress tensor.

How can this be interpreted in terms of physical behavior in the tectonic model? In considering two-dimensional deformation of the lithosphere, the horizontal divergence $u_{\mu,\mu}$ need not in general vanish, this case corresponding to the occurrence of crustal shortening (or extension). While such areal dilatations in the lithospheric plate are resisted by restoring forces, these are not forces which increase without limit as crustal shortening or thickening occur. Rather, these resisting forces are related to the equilibrium height of topography induced by crustal area changes, and for constant (or slowly changing) topographic distributions they are adequately represented by constant (in time) pressure terms (P in equation (2b)).

Thus in this type of lithospheric deformation model, there exists a complete analogy between the Lame parameters of elasticity, λ and μ, and the bulk and shear viscosities λ and η of Newtonian flow. It is thus asserted that given appropriate choices of these parameters and a priori topographic pressure distribution, elastic stress/strain solutions can provide a good approximation to the field of plastic deformation in the lithosphere. Moreover, the parallel work of England and McKenzie (Ref. 5) indicates that the magnitudes of topography-induced stresses are probably such that they do not exert a dominating influence on the pattern of horizontal flow.

A major part of the work reported here consists of such crustal deformation models, which seek to explain spatial variations in stress and strain, as they are observed to occur in Southern California. While such models may be interpreted as giving elastic strains, we emphasize here their interpretation as models of irreversible plastic strain. This remark applies to the following discussion of anisotropic models.

As is emphasized in the work of Ivins et al. (Ref. 6), which has proceeded in collaboration with this work, it may be important in tectonic deformation models to take into account the effect of numerous subparallel minor faults which define a tectonic "fabric" of shear deformation in a given region. The effect of numerous parallel joints or faults is to introduce an effective material anisotropy in the model when treating it as a homogeneous continuum.

Both analytic results and finite element calculations have shown that directional variations in effective shear modulus (or shear viscosity) by factors of ~ 10 occur in media with freely slipping fault densities, which are reasonable for a shear zone like that in the vicinity of the San Andreas fault.

In the case of a general anisotropic body, the matrix of stiffness constants relating stresses and strains (strain rates) contains 21 independent entries. If, however, we restrict ourselves to a two-dimensional case in which the anisotropy takes the form of parallel stratification in material properties (orthotropic plates), four elastic constants are required. In practice, the orthotropic stiffness matrix is evaluated in a coordinate system aligned with the direction of stratification and is subsequently rotated by coordinate transformation into the appropriate model orientation (Ref. 7). The accuracy of anisotropic finite element solutions obtained with this program have been checked by comparison with analytic results, such as those of Lekhnitskii (Ref. 8).

In addition to the above mentioned models of two-dimensional continuum deformation, the work included in this study has also included models of elastic fault interactions. Central to this work has been the development and utilization of "roller" elements for the accommodation of arbitrary slip on a dislocation surface.

Whereas a priori specified fault motions may be input into a model via the split node technique (e.g., Ref. 9), the roller technique described here allows the solution for the fault dislocation as an implicit part of the finite element solution. As Fig. 1 shows schematically, the rollers consist of incompressible bar or "truss" elements which are positioned between pairs of nodes spanning a gap or "crack" in the material grid which represents the fault. In practice, this fault width is made small in comparison with the typical element spacing along its length. For the study of stress relief on a fault, the desired stress drop is applied as tractions on the fault walls. On the other hand, fault creep accompanying regional deformation is modeled by application of boundary conditions to the grid as a whole.

The above descriptions summarize the salient specific techniques in finite element analysis used in the accomplishment of this research. In addition to these developments, work was performed to write a program for automatic finite element grid generation in problems involving roller faults and cracks. This software development effort resulted in the program GRIDX (see Appendix). The following section summarizes the scientific results of the application of the techniques for tectonic modeling so far described.

III. Results and Implications

A. Block Deformation Models and Correspondence with Southern California

A common feature of modern tectonic models of continental regions such as Southern California is the breaking up of such regions into a number of discrete "blocks" within each of which geological and tectonic features are largely homogeneous. One end member in a family of such block tectonic models is of a type described by Hill (Ref. 10). In this picture, blocks interact mainly through frictional forces at block boundaries, and overall regional deformation is accommodated by thrust, normal, and transform slip on the polygonal network of boundary faults.

A contrasting model framework takes the view that continuously distributed deformation occurs throughout the blocks, and that such continuous inelastic deformation makes a major contribution to long-term tectonic motions. In this view, therefore, block boundaries would be largely defined by contrasts in constitutive properties, rather than by the location of major bounding faults, as is the former class.

Clearly, the second type of model also corresponds to slip on discrete faults, if only scrutinized on a small enough scale. The distinction is that the distribution, both in time and space, of fault slip is assumed in this view to be so nearly continuous as to be modeled by continuum deformation. It is perhaps obvious that each of these two extreme views have strengths and weaknesses when compared with reality.

The models from this work seek to correlate features of Southern California tectonics with a continuum deformation model. While geodetic strain rates in California may be strongly perturbed by transient strain associated with great earthquake cycles on the San Andreas, Thatcher (Ref. 11) presents data which suggest that in the southern segment, on which ~ 120 years has elapsed since the last great event, earthquake-related strain has decayed to a low level compared with the average interseismic rate. Thus, distributed shear within ~ 100 km of the main trace of the San Andreas may be a useful model of present-day strain accumulation in the region, as well as explaining the apparent deficit between plate motion rates and geologic slip rates on the main fault.

Figure 2 is a map diagram of Southern California block tectonics, taken from Luyendyk et al. (Ref. 12). Highlighted in this figure are the "transverse" crustal blocks, which in addition to having generally east-west striking fault and structural trends, have experienced large ($\sim 70°$) clockwise block rotations since Miocene time, as determined from paleomagnetism. It is significant for this discussion to note that the "big bend" of the San Andreas fault coincides with its encounter with the western transverse block, and apparently offsets it from its eastern counterpart. This observation provides the point of departure for our discussion of the finite element models.

We consider as the prototypical block model the simple case of an elliptical inclusion in an infinite (two-dimensional) medium. This geometry has the virtue of being amenable to analytic solution in certain cases. All models discussed in this work have the elliptical block with a 3:1 aspect ratio and oriented with the major axis along the abscissa (east-west). Although somewhat arbitrary, this choice yields a geometric similarity with the case of the Southern California Transverse block.

Calculations using simple isotropic material descriptions immediately show that very large contrasts in moduli are required to obtain stress field perturbations of the magnitude implied by the Big Bend and local variations in geodetic strain. Unless order-of-magnitude contrasts in strength between the block and surrounding medium are assumed, the resulting stress field is very nearly homogeneous.

Interestingly, this seemingly implausible requirement of strength contrasts is fulfilled by considering a faulted anisotropic continuum model. As discussed earlier, a 10:1 directional anisotropy in shear stiffness is reasonably accommodated by such a model. Thus, we are led to ask whether judicious choices of crustal anisotropy can lead to plausible patterns of model stress and strain.

Figure 3 presents, in graphical form, the stress (a) and strain (b) fields resulting from a transverse (east-west-faulted) block imbedded in a NW-SE trending faulted medium. The entire model is subjected to uniform pure shear by imposing N-S compressive and E-W tensile stresses at the distant boundaries. Other than differing in grain orientation the two regions have identical properties with 10:1 stiffness ratios. In coordinates for which x lies along the faults, the stiffness constants are given by

$$\begin{bmatrix} \sigma_{xx} \\ \sigma_{yy} \\ \sigma_{xy} \end{bmatrix} = \begin{bmatrix} C_{11} & C_{12} & 0 \\ C_{12} & C_{22} & 0 \\ 0 & 0 & C_{66} \end{bmatrix} \begin{bmatrix} \epsilon_{xx} \\ \epsilon_{yy} \\ \epsilon_{xy} \end{bmatrix} \tag{3}$$

In the isotropic case, $C_{11} = C_{22} = \lambda + 2\mu$, while $C_{66} = \mu$. In the orthotropic case just described, we let C_{66} relax to 0.1 of its isotropic value, leaving all other constants unchanged. It is easily verified that this leads to a material with two "weak

directions" at 90° to one another, normal and parallel to the direction of faulting. The "strong" directions for shear are at 45° to these directions.

The effect of the choice of orientations in Fig. 3 is to shear the "block" along its "strongest" direction while the surrounding medium shears along its most compliant direction. Immediately evident in the stress plot is a symmetric pattern of rotation in the orientation of principal stresses around the periphery of the inclusion (the plots show the directions and magnitudes of principal stresses/strains, with outward directed heads denoting extension). The sense of rotation is clockwise in the NW and SW. The sense of stress is predominantly compressive along the north and south sides of the inclusion, and tensile at the "ends." Accentuated east-west tensile stresses also characterize the block interior, where there is no rotation in orientation.

The plot of model strains (or strain rates in the visous interpretation) shows a somewhat different picture. No strong pattern of differential rotations is seen as in the stress plot. Aside from a slight global clockwise rotation, the strain directions are not influenced by the block. Although the stress field shows significant regions of compressive stress, the net effect in this model is *not* to produce any significant crustal shortening, as all observed *strains* are either isovolumetric, or slightly extensional.

In Fig. 4, adapted from Savage et al. (Ref. 13) geodetically measured strain rates in Southern California are shown along with a suggested analogy between the Western Transverse block and the elliptical inclusion model. Since this correspondence places much of the block's western end in the ocean, all the geodetic results apply to the eastern half of the model.

These USGS trilateration results show a general correspondence with the rotation of stresses in the model. In the NE quadrant (Tehachapi/Palmdale, for example) strain orientations are rotated counterclockwise along with the fault strike of the Big Bend. SE quadrant networks (e.g., Anza) appear to show a slight clockwise complementary rotation, relative to the direction of shear in the more distant Salton network.

This apparent success of the simple inclusion model is not satisfactory for a number of reasons. First, and perhaps most important, the model predicts rotation of stresses but not strains, which are the observed quantities. In addition, the finite element model displays a marked degree of symmetry (because of its symmetry of boundary conditions), which may not be reflected in the real situation. Whereas the model is formally indifferent as to whether the deformation is primarily right lateral on NW trending structures, or left lateral on NW trends, the actual tectonics of Southern California is manifestly dominated by dextral shear. The predominance of clockwise block rotations and counterclockwise strain axis rotations in conjunction with the Big Bend reflect this fundamental asymmetry.

Figure 5 gives the strain field resulting from modifying the finite element model to more realistically represent the actual situation. In this model, rather than imbedding the inclusion in a faulted medium of infinite extent, the anisotropic medium is confined to a NW-SE trending band or "shear zone," just wide enough to contain the elliptical block. Outside this band, the material has the isotropic properties of unfaulted material ($C_{66} = 1/3\ C_{11}$). Besides more accurately emulating the zone of diffuse shear deformation which surrounds the San Andreas Fault, this modification has two evident effects on the pattern of deformations (or flow). First, it effectively "channels" deformation, restricting it to regions which must interact with the inclusion. This has the effect of amplifying the perturbing effect of the block on strains, which were formerly only weakly affected. Secondly, the presence of the diagonal channel introduces a preferred direction in the model, thus providing a basis for breaking the symmetry of the earlier solutions.

The results of this model are to bring the strain field into somewhat better agreement with our expectations of the real situation. As expected, shear strain amplitudes are enhanced in the channel relative to the outer regions. Also, the orientation of the principal strains is rotated slightly counterclockwise in the NE quadrant, in agreement with the location and sense of fault strike and strain rotation in the Big Bend region. This rotation no longer has a complementary opposite rotation in the NW quadrant in this unsymmetric model, although it does predict comparable counterclockwise rotations in the SW quadrant. This prediction of the anisotropic block model could in principle be checked by geodetic network measurements in the Channel Islands region.

While the qualitative pattern of strain distributions is improved in this channel model, the magnitude of rotations predicted is quantitatively small compared with the strike rotation observed on the San Andreas. This in turn suggests that further narrowing of the channel could be used to obtain closer agreement. The suggestion that the shear zone may be actually narrower than the proto-Transverse Ranges block receives some support from reconstructions, such as those of Luyendyk et al. (Ref. 12) which suggest that the offset eastern and western Transverse blocks formed a single unit prior to the inception of motion on the modern (bent) trace of the San Andreas fault.

In Fig. 6, the modeled situation is as in Fig. 5, except that the shear zone now has a width of about 40% of that of the

inclusion major axis (the ratio of widths projected along the fault strike is 56%). As anticipated, large amplitude strain rotations are obtained in a fairly narrow boundary zone coincident with the interpreted position of the fault bend. Evidently, this rotation is a sensitive function of shear zone width, and within the context of this model, suggests that the actual situation in Southern California should be modeled with a shear band approximately 100-150 km in width. In reality, the transition from "weak" faulted medium to more nearly isotropic crustal material is probably gradational, rather than steplike as in this simple model. Therefore, this 100-150 km scale might be regarded as a "halfwidth" of distributed shear deformation in the diffuse plate boundary region. This agrees fairly well with the lateral extent of strike slip faulting in the Salton trough and surrounding regime.

As has been emphasized above, the models considered thus far represent generalized pictures of certain processes which may be important in determining the overall tectonic pattern in specific regions, such as Southern California. It is through the methodical construction of such "long-wavelength" tectonic models that progress is made toward meaningfully modeling the tectonics of the real situation on finer spatial scales. The areas in which future research promises to further the achievement of this goal include consideration of gradients in constitutive properties (which may be inferred from geologic fault-slip data), and the relative influence of topographic stresses in controlling secular deformation. In the remainder of this report, we discuss modeling problems of finer scale, examining the interactions of small numbers of faults and their immediate local effects.

B. Seismic Gap Fault Models and Applications to Anza, California

The states of stress and strain occurring near the focal region of an impending earthquake are of great importance for studies of earthquake prediction. Information of this kind may come from a variety of sources, including seismological, geodetic, and in situ monitoring. The finite element method offers the potential of modeling these results in situations where geometric or geologic complexities may be important influences. During this study, attention has been focused upon the inferred seismic gap near Anza, California, in which the occurrence of a magnitude 5 earthquake is considered likely.

Figure 7 shows a map of the region of the San Jacinto fault near Anza. Plotted are the surface traces of mapped faults, with major active strands of the San Jacinto shown as heavy lines. Small crosses show the epicenter locations of earthquakes with $M > 2$ between January 1977 and July 1981. The seismic "gap" is visible here as a paucity of small earthquakes between the outlined strands of the fault. The relative absence of events extends uniformly to ~ 20 km depth, where all seismicity ceases. The seismological data for this world have come from Sanders et al. (Ref. 14).

The evidence for anomalous stress in this gap region comes from the two small earthquake swarms indicated on Fig. 7. Focal mechanism studies of these events show a consistent clockwise rotation of the inferred axis of maximum compression, from its expected north-south azimuth. The effect is larger for the swarm closest to the fault, and in that case amounts to about a 20° clockwise rotation of stress axes.

The goal of finite element modeling in this study has been to determine whether this indication of anomalous stress may be understood in terms of strain accumulation on the "locked" segment of the fault, or other processes associated with the seismic gap. Figure 8 is typical of plane stress models constructed for this region. The faults indicated by heavy lines have been modeled as freely slipping dislocations (using the "roller" elements) within an elastic continuum. Principal stresses are plotted, and as before, boundary loading of the problem is achieved with application of surface forces to yield pure shear parallel to the fault strike, in the absence of any perturbing stresses.

In such models, it is found that appreciable stress field rotation occurs, but only relatively near the tips of the modeled dislocations. As may be seen, clockwise rotations of the observed magnitude occur just south of the northwest strand of the fault; however, within the gap, corresponding to the locations of the anomalous swarms, essentially no rotation is obtained. This result remains qualitatively unchanged as we consider, in more detail, different combinations of slipping fault strands outside the locked gap.

Several approaches were tried to obtain models in which the region of rotated stress axes was drawn out into the gap. Among these was a set of models based upon the conjecture that nonlinear effects preceding seismic failure (such as strain hardening or dilatancy) might introduce a zone of anomalous elastic properties within the gap. The results of such models have been uniformly negative, with the finding that even large contrasts in elastic moduli within an elongated body centered on the gap fail to modify the orientation of stresses.

In further work, it was suggested that significant asymmetry might be necessary in the models in order to obtain a preponderance of clockwise rotation over the otherwise symmetric field. Using mapped geological contrasts across the San Jacinto Fault as a general guide, lateral variations in constitutive properties were included in the elastic gap models. Once again, no plausible distribution of material contrasts across the fault(s) provided significant rotations.

The possibility of anisotropy providing an answer, as in the case of the larger scale regional models discussed above, is unsatisfactory for a number of reasons. First of all, in this model configuration, the stress field is found to be dominantly influenced (in the near field) by the major modeled faults. Such models when calculated, yield little or no improvement of the rotation picture.

It could be argued that if anisotropy were important, that the direction of compression and tension axes derived from earthquake focal mechanisms would reflect increments in strain (displacement field) rather than stress. If true, it would indeed be easier to obtain agreement between the strain field and the observed mechanisms. However, this would mean simply assuming ad hoc that a region of strong anisotropy of just the right orientation exists within the gap, and nowhere else. This makes for a very unconvincing and unsatisfying physical model, in light of its arbitrary nature. Moreover, even though we have argued for the existence of strong crustal anisotropy for deformation on *long* time scales, there exists no observational evidence for anisotropy on seismic time scales of the magnitude required for this purpose.

As a general conclusion, it appears difficult to explain the observed stresses as a direct result of rigidly locking the quiet segment of the fault. It may be worthwhile to consider, however, a different physical model for the seismic gap. In particular, we consider the description of this gap as a "geometric asperity," in which a bend or kink in the fault zone inhibits uniform slip locally.

In a left-stepping (dextral sense of slip) kink of the kind illustrated in the model of Fig. 9, compressive stresses are generated in the bent region. These large compressive stresses could provide an increase in internal friction, thus locally inhibiting shear failure and producing a seismically quiet gap. Most importantly, careful examination of Fig. 9 shows that modest clockwise axis rotations occur near the center of the asperity.

While this model enjoys some success in explaining stress rotations, it makes no prediction (except indirectly) about the relation between rotation magnitudes and the likelihood of eventual failure in the geometrically hindered gap. Elucidation of this question will require the consideration of cases in which a friction model determines the transition from locked to sliding fault segments. Ultimately, the glaring weakness of this hypothesis for explaining the observations is that there is no evidence from the morphology of the relevant faults or the distribution of seismicity that any left-stepping fault kink of the kind required actually exists. Unless geophysical data suggesting the occurrence of such a bend are forthcoming, this model agreement must remain an interesting but probably irrelevant coincidence.

In the absence of any compelling explanation for the observations described, we report to the consideration of possible alternatives. It is possible, but difficult, to verify that the observed behavior is due to an anomalous region of preferentially assigned preexisting fractures, which give rise to the observed axes. In this case, the rotated stresses have nothing to do (directly) with the potential for seismicity in the gap, and their association is coincidental. Alternatively, some more subtle aspect of the time-dependent accumulations of stress and strain in the gap needs to be addressed in the finite element model. This is the current state of our understanding of this problem, and new answers await either renewed efforts in modeling, or further geophysical data on the Anza region, or both.

References

1. Melosh, H. J., and Raefsky, A., "Anelastic Response of the Earth to a Dip Slip Earthquake," *J. Geophys. Res., 88*, 515-526, 1983.
2. Yang, M., and Toksoz, M. N., "Time Dependent Deformation and Stress Relaxation after Strike Slip Earthquakes," *J. Geophys. Res.*, 86, 2889-2901, 1981.
3. Cohen, S. C., "Postseismic Rebound Due to Creep of the Lower Lithosphere and Asthenosphere," *Geophys. Res. Lett*, 8, 493-496, 1981.
4. Bathe, K. J. and Wilson, E. L., *Numerical Methods in Finite Element Analysis*, Prentice-Hall, Englewood Cliffs, New Jersey,1976.
5. England, R., and McKenzie, D., "A Thin Viscous Sheet Model for Continental Deformations," *Geophys. J. R Astr. Soc. 70*, 295-321, 1982.
6. Ivins, E. R., Lyzenga, G. A., Sanders, R. S., and Raefsky, A., "Mechanics of the Neogene Rotation of the Transverse Ranges, California," in preparation 1983.
7. Zienkiewicz, O. C., *The Finite Element Method*, McGraw-Hill, London, 1977.
8. Lekhnitskii, S. G. (translated by S. W. Tsai and T. Cheron) *Anisotropic Plates*, Gordon and Breach Publishers, 1968.
9. Melosh, H. J., and Raefsky, A., "A Simple and Efficient Method for Introducing Faults into Finite Element Computations," *Bull. Seismol., Soc. Am., 71*, 1391-1400, 1981.
10. Hill, D. P., "Contemporary Block Tectonics: California and Nevada," *J. Geophys. Res., 87*, 5433-5450, 1982.
11. Thatcher, W., "Nonlinear Strain Buildup and the Earthquake Cycle on the San Andreas Fault," preprint submitted (1983).
12. Luyendyk, B. P., Kamerling, M. J., and Terres, R., "Geometric Model for Neogene Crustal Rotations in Southern California," *Geol. Soc. Am. Bull., 91*, 211-217, 1980.
13. Savage, J. C., Prescott, W. H., Lisowski, M., and King, N. E., "Strain Accumulation in Southern California, 1973-1980," *J. Geophys. Res.*, 86, 6991-7001, 1981.
14. Sanders, C., McNally, K., and Kanamori, H., "The State of Stress near the Anza Seismic Gap, San Jacinto Fault Zone, Southern California," *Trans. Am. Geophys. U.*, 61, 957 (1981).

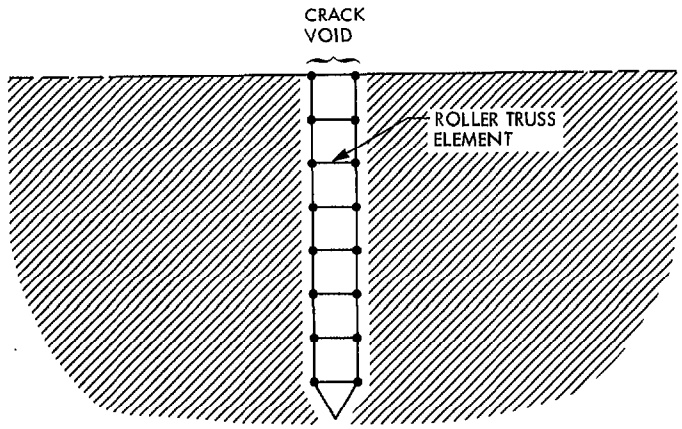

Fig. 1. Schematic representation of roller elements used to model a slipping dislocation in faulted model

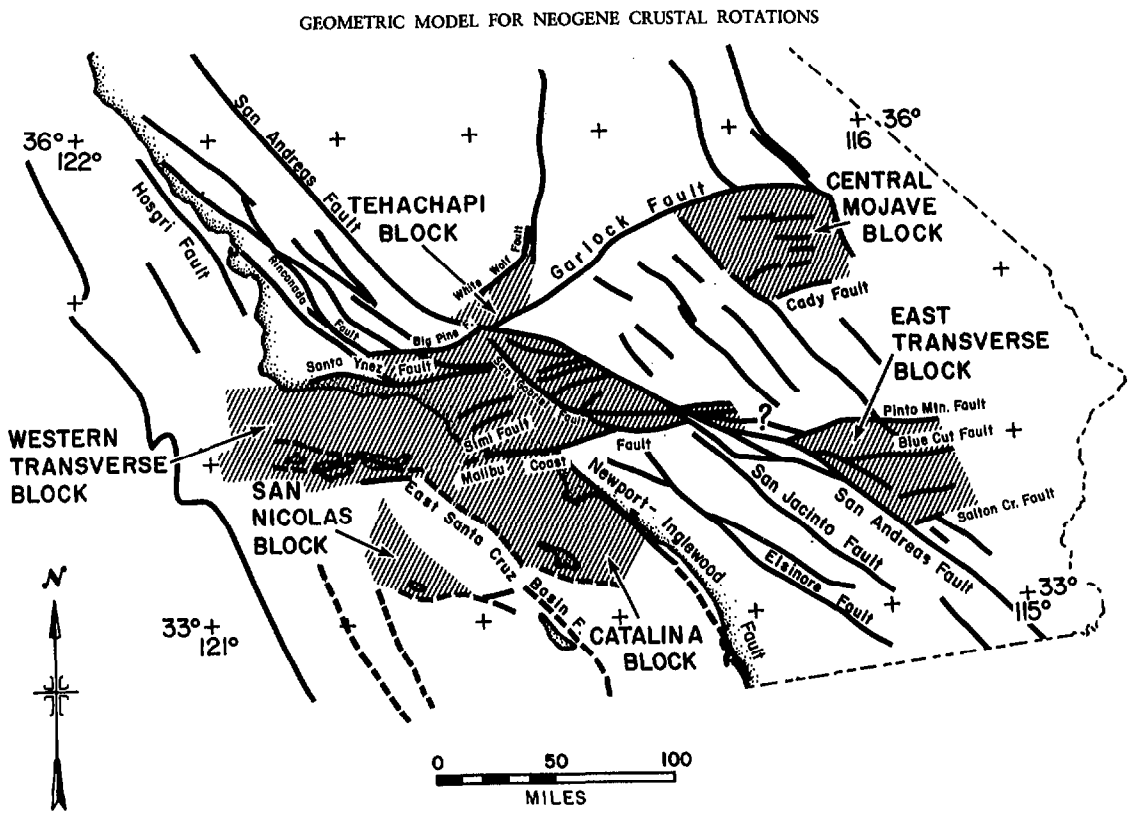

Fig. 2. Map from Luyendyk et al. (Ref. 12) showing Southern California faults and tectonic blocks, for some of which rotations have been inferred from paleomagnetic data

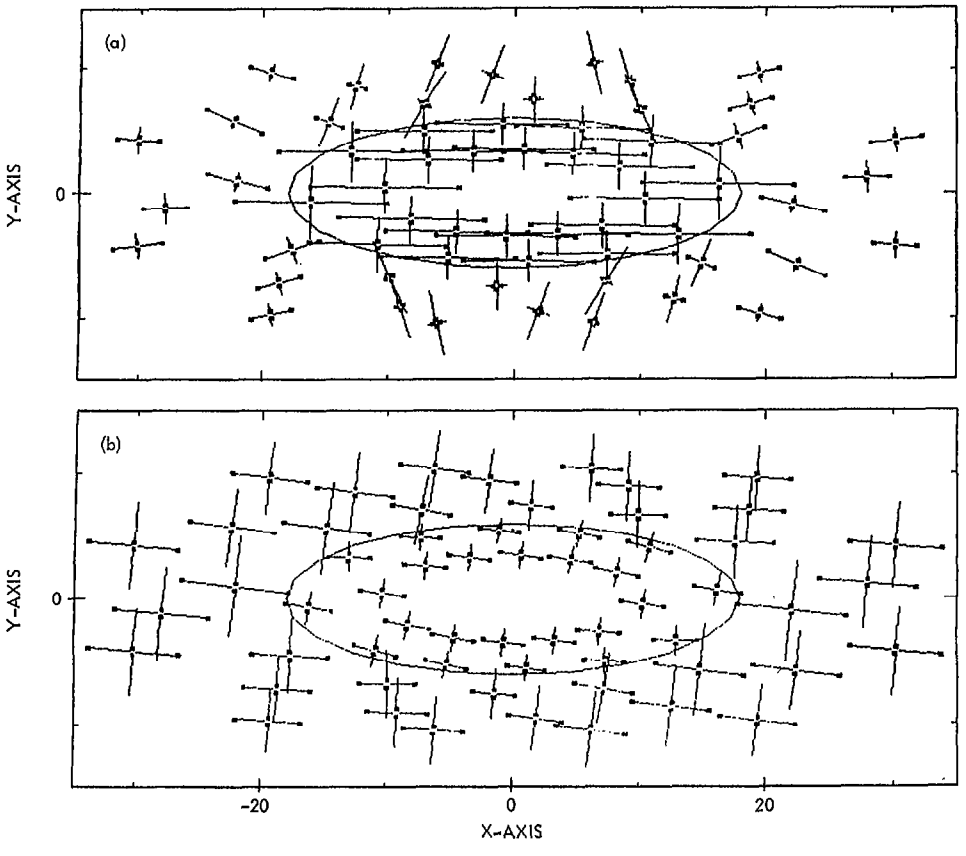

Fig. 3. (a) Stress field obtained in finite element model with anisotropic faulted block whose grain is rotated with respect to surrounding medium orientation; (b) strain field for same model.

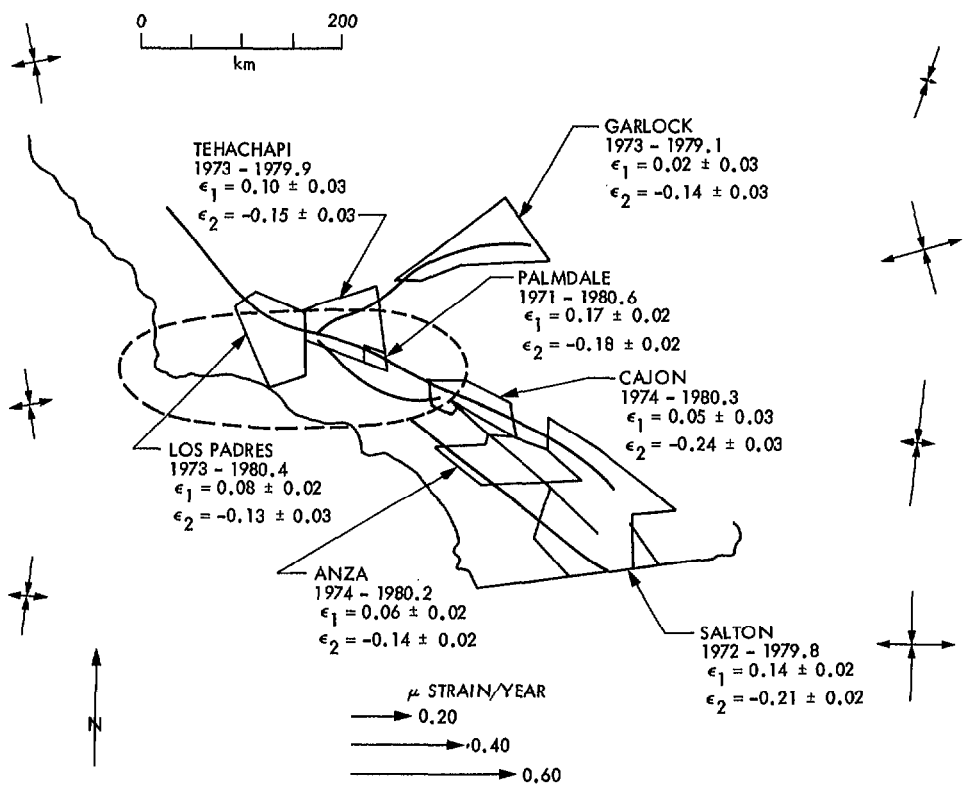

Fig. 4. Map from Savage et al. (Ref. 13) showing measured strain accumulation in Southern California near inferred Transverse block (dashed line)

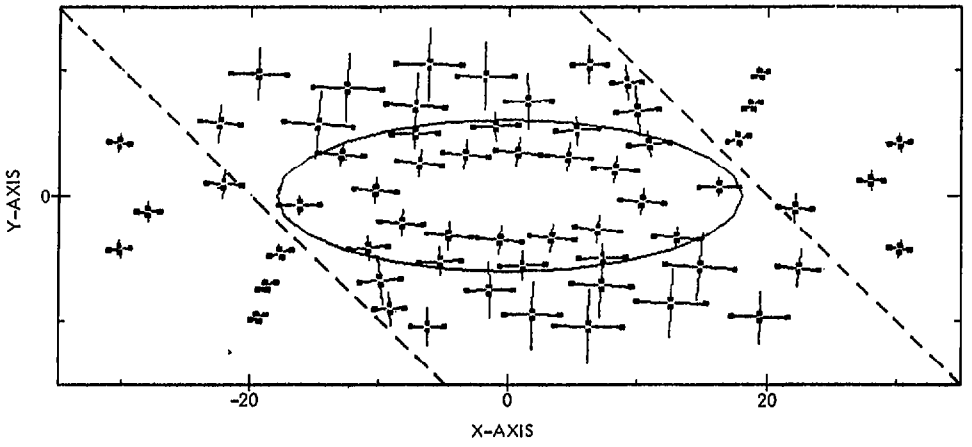

Fig. 5. Strain field in model for which anisotropy in surrounding medium is restricted to a "channel" (dashed line)

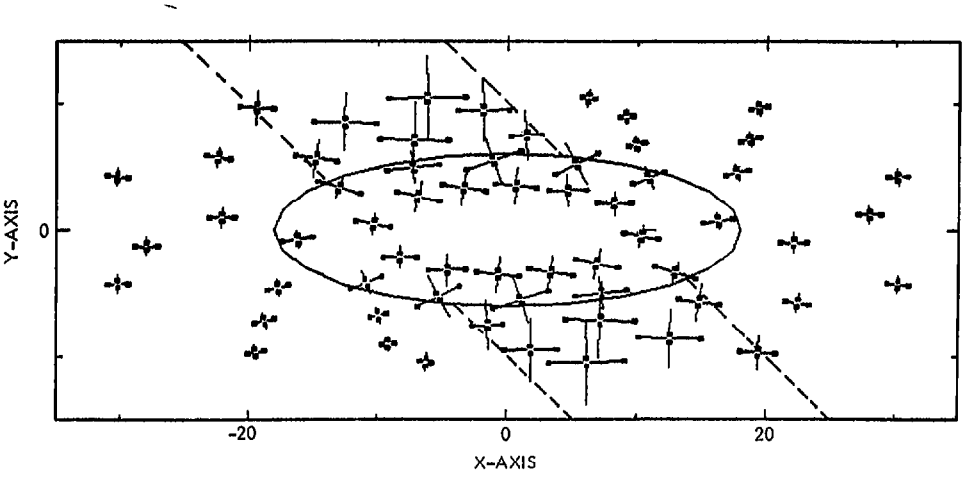

Fig. 6. Strains for channel model as in Fig. 5, but with channel width one half that of the previous case

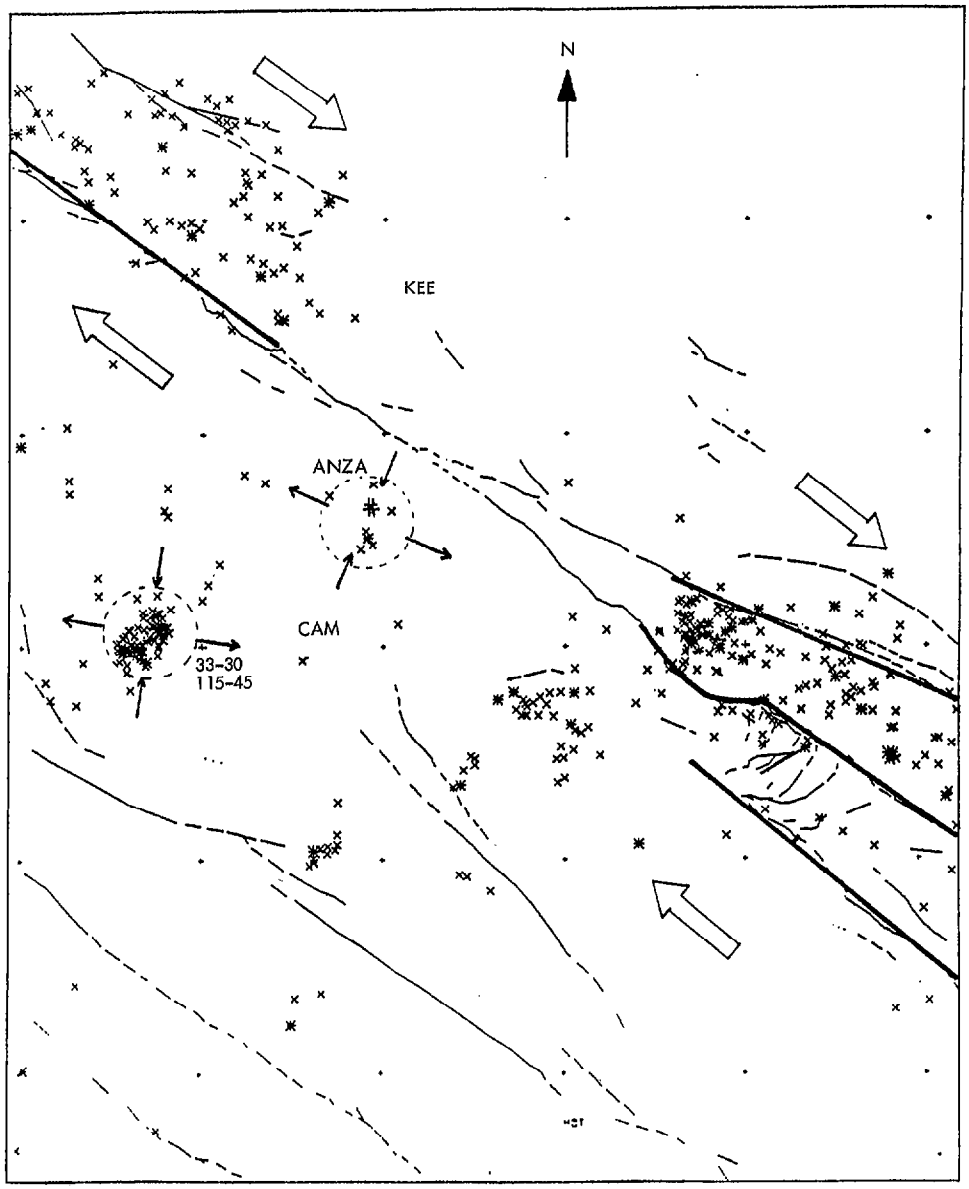

Fig. 7. Map of Anza region, showing distribution of seismicity, mapped faults, and orientation of stress axes for two anomalous swarms of earthquakes. Data taken from work of Sanders et al. (Ref. 14)

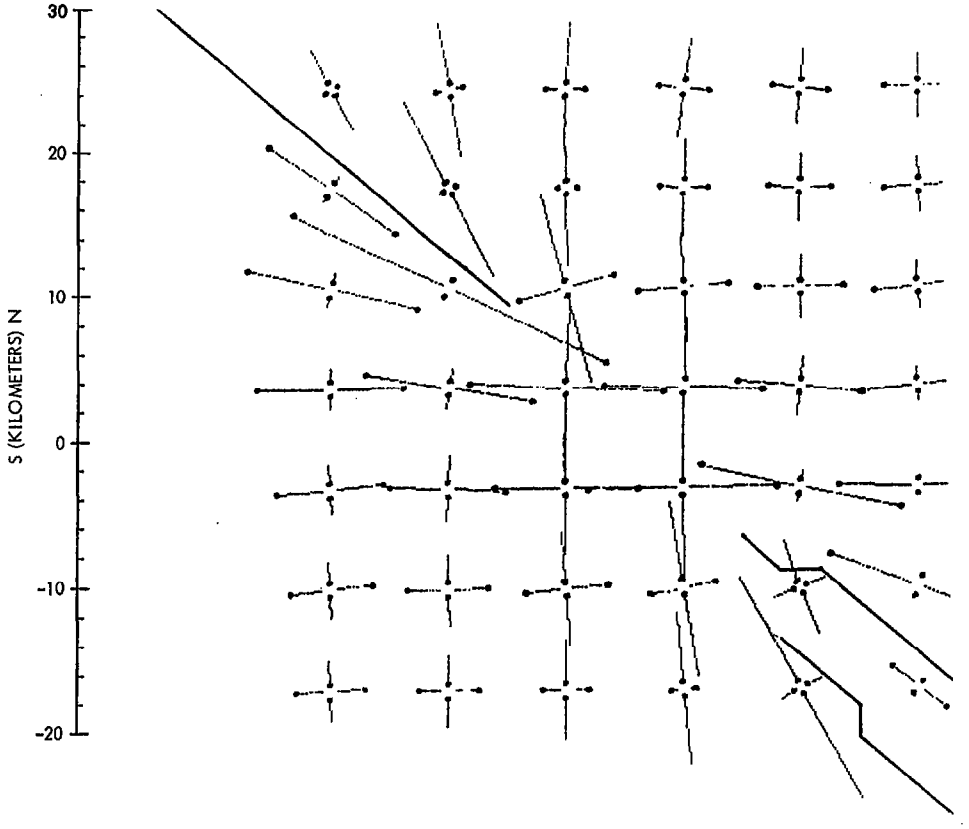

Fig. 8. Elastic dislocation model of stress field in vicinity of a locked fault gap with shown distribution of active faults (heavy lines)

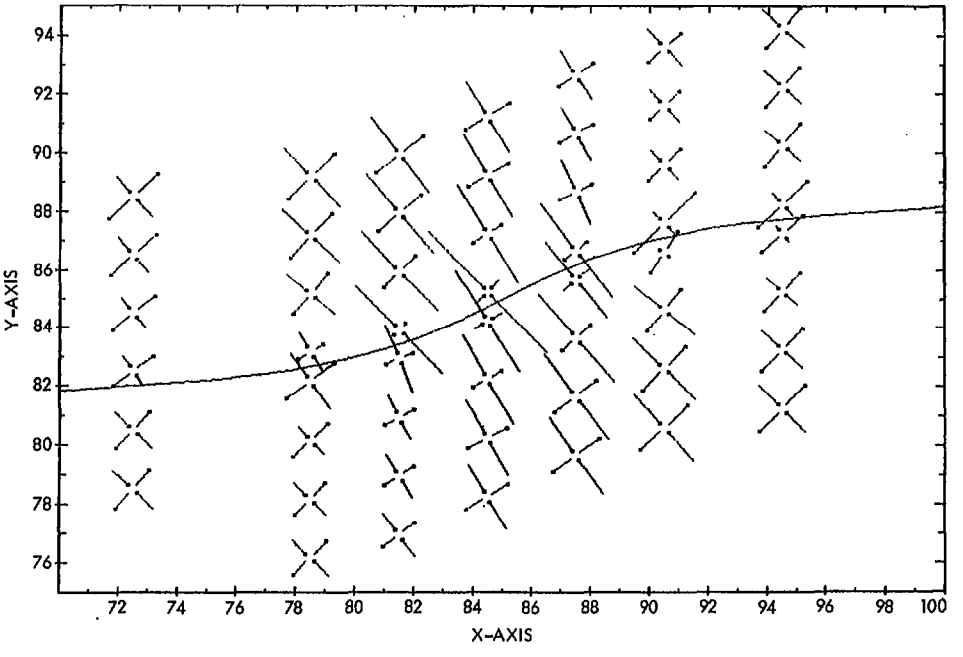

Fig. 9. Stress distribution near left-stepping bend in an elastic fault model for a geometric asperity

Appendix

Brief Descriptive Summary of Program GRIDX

The following is a brief description of the purpose and use of FORTRAN program GRIDX. This program was developed to provide a utility for the generation of complex finite element computational grids incorporating faults, as are required in many tectonics problems. GRIDX is intended as a flexible routine for the generation of nodal coordinates and element global node assignment (IEN array), with a simplified input format. A listing and detailed description of GRIDX is available from G. Lyzenga (JPL, extension 6920).

Input to GRIDX consists of parameters which control the size and spacing of elements in a rectangular grid. Following this input, the program accepts codes describing the boundary conditions to be applied to the particular problem. Finally, input is read which generates fault roller elements of the required spacing and orientation to model faults. The input of a few lines of generation parameters allows the immediate assembly of a finite element grid and all the necessary nodal information for a complex grid which would require many hours to assemble and number manually.

Output from GRIDX is provided in two forms. The first and most important is the output file, containing the nodal coordinates and numbering, as well as the boundary conditions and element arrays in ready-to-use format for the finite element program. Secondly, the program provides (optionally) a plot display of the generated grid in order to provide the user with easy verification that the desired grid has been properly generated. The program is intended to be generally applicable to the types of problems discussed in this report, but is also adaptable to other finite element modeling or software requirements.

NASA—JPL—Coml., L.A., Calif.